AIMS Mathematics, 10(9): 21040–21060.
DOI: 10.3934/math.2025940
Received: 18 June 2025
Revised: 28 August 2025
Accepted: 01 September 2025
Published: 12 September 2025

https://www.aimspress.com/journal/Math

Research article

A sixth-order compact finite difference framework for solving nonlinear reaction-diffusion equations: application to FitzHugh-Nagumo model

Jiang Fu[1], **Xiao-Yu Zhang**[1,*] **and Qing Fang**[2]

[1] Department of Mathematics, College of Science, Beijing Forestry University, Beijing, 100083, China

[2] Department of Mathematical Sciences, Faculty of Science, Yamagata University, Yamagata, 990-8560, Japan

* **Correspondence:** Email: xyzhang@bjfu.edu.cn.

Abstract: This paper proposes a sixth-order compact finite difference framework to numerically solve nonlinear reaction-diffusion equations, with a particular focus on the FitzHugh-Nagumo (FHN) model. First, for the second-order spatial derivatives in the FHN equation, a five-point sixth-order compact difference scheme is used for internal points, and a asymmetric six-point compact difference scheme is used for boundary points to achieve spatial discretization, thereby transforming the problem into an ordinary differential equation; then, this is and then combined with the semi-implicit Crank-Nicholson method for the time discretization to obtain a numerical solution scheme for the FHN equation. We establish the stability and convergence of the method and validate it through numerical experiments. The feasibility and accuracy of the method were verified by conducting an error analysis on the numerical results and comparing them with other algorithms. It is proven that this method is an effective tool to solve the numerical solutions of nonlinear reaction-diffusion equations.

Keywords: FitzHugh-Nagumo equation; nonlinear reaction-diffusion equation; numerical method; compact finite difference method; Crank-Nicolson method
Mathematics Subject Classification: 35K57, 65M06, 65M12

1. Introduction

The FitzHugh-Nagumo (FHN) equation is an important nonlinear reaction diffusion equation and a classical model used in neuroscience to describe the impulse behavior of neurons. Based on its excitation-recovery and non-linear properties, it has also been widely used in fields such as neurophysiology [1, 2], circuit theory [3], branching Brownian motion processes, logistic population growth, nuclear reactor theory [4], and autocatalytic chemical reactions.

Consider the following FHN equation:

$$\frac{\partial u}{\partial t} = \frac{\partial^2 u}{\partial x^2} + u(1-u)(u-\theta), \quad p \le x \le q,\ 0 \le t \le T, \tag{1.1}$$

with the initial conditions

$$u(x,0) = u_0(x), \quad p \le x \le q, \tag{1.2}$$

and the boundary conditions

$$u(p,t) = f_1(t), u(q,t) = f_2(t), \quad 0 \le t \le T, \tag{1.3}$$

where $\theta \in (0,1)$, and $u(x,t)$ is an unknown function that depends on the time variable t and the space variable x. In particular, when $\theta = -1$, Eq (1.1) reduces to the real Newell-Whitehead equation, which describes the dynamical behavior near the bifurcation point for the Rayleigh-Benard convection of binary fluid mixtures.

The FHN equation originated from a simplification of the Hodgkin-Huxley model, and was initially used as a simplified model to describe the excitatory conduction behavior of neurons; the equation was proposed by FitzHugh [5] and improved by Nagumo [6] to form the classical FHN model. Since then, the equation has been extensively studied and applied. Because the problem of not having an exact solution or the exact solution being difficult to obtain is often encountered in practice, high-precision numerical algorithms have been a hotspot of researchers' attention in recent years.

There are many studies on the numerical solution of the FHN equation. Hariharan et al. [7] introduced the Haar wavelet method to solve the FHN equation, and Namjoo et al. [8] provided a numerical solution of the FHN equation based on a nonstandard finite difference format. Shekarabi et al. [9] constructed a three-time-level implicit method using the tensor spline function. İnan [10, 11] proposed the Crank-Nicolson exponential finite difference method to solve the FHN equation [10], as well as an improved explicit exponential finite difference method using the Padé approximation technique [11]. Al-Juaifri et al. [12] proposed the numerical approximation of the FHN system based on the finite element method, which provides the bounds of the numerical solution. Agbavon et al. [13] constructed a series of non-standard finite difference formats to solve FHN equations with specified initial and boundary conditions in different cases. Hilal et al. [14] proposed the implicit exponential finite difference method and the fully implicit exponential finite difference method to compute numerical solutions of the Newell-Whitehead-Segel equation. Fan et al. [15] used the residual power series method (RPSM), the homotopy perturbation method (HPM), and a modified fractional Taylor expansion to solve the FHN equations.

Lele [16] proposed a class of compact finite difference formats to approximate the second-order derivatives over a range of spatial scales, but did not apply them to nonlinear partial differential equations. In this paper, we apply the sixth-order accuracy format from the reference [16] to the spatial region of the discretized FHN equation, and then use the Crank-Nicolson method to discretize the time region of the FHN equation, and construct a new Compact finite difference method to solve the FHN equation. The numerical results show that the method has the advantages of easy implementation and high accuracy.

2. Spatial discretization

We divide the spatial region into equidistant grids and construct $M+1$ points to equally divide the interval $[p,q]$; we denote these points as follows:

$$x_i = p + (i-1)h \quad (1 \le i \le M+1,\ h = \frac{p-q}{M}).$$

We denote the symbols as follows:

$$u_i^j = u(x_i, t_j),\ u_i = u(x_i, t),\ u_i' = \frac{\partial u}{\partial x}(x_i, t),\ u_i'' = \frac{\partial^2 u}{\partial x^2}(x_i, t).$$

For internal points, we use a five-point sixth-order compact difference scheme.

Let the second order derivative of u with respect to x have the following approximation:

$$\beta u_{i-2}'' + \alpha u_{i-1}'' + u_i'' + \alpha u_{i+1}'' + \beta u_{i+2}'' = a\frac{u_{i+1} - 2u_i + u_{i-1}}{h^2} + b\frac{u_{i+2} - 2u_i + u_{i-2}}{4h^2} + c\frac{u_{i+3} - 2u_i + u_{i-3}}{9h^2}, \quad (2.1)$$

where α, β, a, b and c are constants to be determined.

Expand $u_{i\pm1}$, $u_{i\pm2}$, $u_{i\pm3}$, $u_{i\pm1}''$, and $u_{i\pm2}''$ into the Taylor series at $x = x_i$, substitute them into Eq (2.1), and then compare the coefficients of the Taylor series at different orders to obtain the following:

$$a + b + c = 1 + 2\alpha + 2\beta \quad \text{(second order)},$$

$$a + 2^2 b + 3^2 c = 12(\alpha + 2^2\beta) \quad \text{(fourth order)},$$

$$a + 2^4 b + 3^4 c = 30(\alpha + 2^4\beta) \quad \text{(sixth order)},$$

$$\cdots$$

The more equations that the undetermined constants α, β, a, b and c satisfy, the smaller the formal truncation error of the approximation, and the last satisfied equation determines the formal truncation error of the approximation.

Consider the following system of equations:

$$\begin{cases} a + b + c = 1 + 2\alpha + 2\beta, \\ a + 2^2 b + 3^2 c = 12(\alpha + 2^2\beta), \\ a + 2^4 b + 3^4 c = 30(\alpha + 2^4\beta). \end{cases} \quad (2.2)$$

Let $c = \beta = 0$; solve $a = \frac{12}{11},\ b = \frac{3}{11},\ \alpha = \frac{2}{11}$, and then obtain the second derivative approximation with the sixth-order truncation error at the inner points x_i $(i = 3, 4, \cdots, M-1)$ as follows:

$$\frac{2}{11}u_{i-1}'' + u_i'' + \frac{2}{11}u_{i+1}'' = \frac{1}{h^2}(\frac{3}{44}u_{i-2} + \frac{12}{11}u_{i-1} - \frac{51}{22}u_i + \frac{12}{11}u_{i+1} + \frac{3}{44}u_{i+2}), \quad (2.3)$$

where $i = 3, 4, \cdots, M-1$.

For the boundary points at x_1 and x_2, we use an asymmetric six-point compact difference scheme. Let the derivative of u with respect to x at x_1 and x_2 have the following approximation:

$$u_1'' + \alpha u_2'' = \frac{1}{h^2}(au_1 + bu_2 + cu_3 + du_4 + eu_5 + fu_6). \quad (2.4)$$

Expand u_2'', u_2, u_3, u_4, u_5, and u_6 into the Taylor series at $x = x_1$, substitute them into Eq (2.4), and then compare the coefficients of the Taylor series at different orders to obtain the following:

$$\begin{cases} a + b + c + d + e + f = 0, \\ b + 2c + 3d + 4e + 5f = 0, \\ b + 2^2c + 3^2d + 4^2e + 5^2f = 2(\alpha + 1), \\ b + 2^3c + 3^3d + 4^3e + 5^3f = 6\alpha, \\ b + 2^4c + 3^4d + 4^4e + 5^4f = 12\alpha, \\ b + 2^5c + 3^5d + 4^5e + 5^5f = 20\alpha, \\ b + 2^6c + 3^6d + 4^6e + 5^6f = 30\alpha. \end{cases}$$

By solving, we obtain the following:

$$\alpha = \frac{137}{13},\ a = \frac{1955}{156},\ b = -\frac{4057}{156},\ c = \frac{1117}{78},\ d = -\frac{55}{78},\ e = -\frac{29}{156},\ f = \frac{7}{156}.$$

Thus, we obtain the following second derivative approximation scheme with a sixth-order truncation error at the boundary points x_1 and x_2:

$$u_1'' + \frac{137}{13}u_2'' = \frac{1}{h^2}(\frac{1955}{156}u_1 - \frac{4057}{156}u_2 + \frac{1117}{78}u_3 - \frac{55}{78}u_4 - \frac{29}{156}u_5 + \frac{7}{156}u_6). \tag{2.5}$$

Similarly, at the boundary points x_M and x_{M+1}, we have the following:

$$\frac{137}{13}u_M'' + u_{M+1}'' = \frac{1}{h^2}(\frac{1955}{156}u_{M+1} - \frac{4057}{156}u_M + \frac{1117}{78}u_{M-1} - \frac{55}{78}u_{M-2} - \frac{29}{156}u_{M-3} + \frac{7}{156}u_{M-4}).$$

We summarize the spatial difference schemes as follows:

$$\begin{cases} u_1'' + \frac{137}{13}u_2'' = \frac{1}{h^2}(\frac{1955}{156}u_1 - \frac{4057}{156}u_2 + \frac{1117}{78}u_3 - \frac{55}{78}u_4 - \frac{29}{156}u_5 + \frac{7}{156}u_6), \\ \frac{2}{11}u_{i-1}'' + u_i'' + \frac{2}{11}u_{i+1}'' = \frac{1}{h^2}(\frac{3}{44}u_{i-2} + \frac{12}{11}u_{i-1} - \frac{51}{22}u_i + \frac{12}{11}u_{i+1} + \frac{3}{44}u_{i+2}) \ \ (i = 3, 4, \cdots, M-1), \\ \frac{137}{13}u_M'' + u_{M+1}'' = \frac{1}{h^2}(\frac{1955}{156}u_{M+1} - \frac{4057}{156}u_M + \frac{1117}{78}u_{M-1} - \frac{55}{78}u_{M-2} - \frac{29}{156}u_{M-3} + \frac{7}{156}u_{M-4}). \end{cases}$$

3. Time discretization

We divide the temporal region into equidistant grids and construct N+1 points to equally divide the interval $\left[0, T\right]$; we denote these points as follows:

$$t_j = (j-1)\Delta t \quad (1 \le j \le N+1,\ \Delta t = \frac{T}{N}).$$

According to Eq (2.3), at the interior points x_i ($i = 3, 4, \cdots, M-1$), we have the following:

$$\begin{aligned} &\frac{2}{11}\frac{\partial u}{\partial t}|_{x=x_{i-1}} + \frac{\partial u}{\partial t}|_{x=x_i} + \frac{2}{11}\frac{\partial u}{\partial t}|_{x=x_{i+1}} \\ &= \frac{2}{11}u_{i-1}'' + u_i'' + \frac{2}{11}u_{i+1}'' + \frac{2}{11}\varphi(u)|_{x=x_{i-1}} + \varphi(u)|_{x=x_i} + \frac{2}{11}\varphi(u)|_{x=x_{i+1}} \\ &= \frac{1}{h^2}\left(\frac{3}{44}u_{i-2} + \frac{12}{11}u_{i-1} - \frac{51}{22}u_i + \frac{12}{11}u_{i+1} + \frac{3}{44}u_{i+2}\right) + \frac{2}{11}\varphi(u)\ |_{x=x_{i-1}} + \varphi(u)\ |_{x=x_i} + \frac{2}{11}\varphi(u)\ |_{x=x_{i+1}}, \end{aligned}$$

where $\varphi(u) = u(1-u)(u-\theta)$. For convenience, we denote $\varphi_i^j = \varphi(u)\,|_{x=x_i}^{t=t_j}$.

Using the Crank-Nicolson scheme in time, we obtain the following:

$$\begin{aligned}
&\frac{2}{11}\frac{u_{i-1}^{j+1}-u_{i-1}^{j}}{\Delta t}+\frac{u_{i}^{j+1}-u_{i}^{j}}{\Delta t}+\frac{2}{11}\frac{u_{i+1}^{j+1}-u_{i+1}^{j}}{\Delta t}\\
&=\frac{1}{2h^2}[(\frac{3}{44}u_{i-2}^{j+1}+\frac{12}{11}u_{i-1}^{j+1}-\frac{51}{22}u_{i}^{j+1}+\frac{12}{11}u_{i+1}^{j+1}+\frac{3}{44}u_{i+2}^{j+1})\\
&\quad+(\frac{3}{44}u_{i-2}^{j}+\frac{12}{11}u_{i-1}^{j}-\frac{51}{22}u_{i}^{j}+\frac{12}{11}u_{i+1}^{j}+\frac{3}{44}u_{i+2}^{j})]+\frac{2}{11}\varphi_{i-1}^{j}+\varphi_{i}^{j}+\frac{2}{11}\varphi_{i+1}^{j}.
\end{aligned}$$

After simplification, the internal difference format is obtained as follows:

$$\begin{aligned}
&-\frac{3}{88}su_{i-2}^{j+1}+(\frac{2}{11}-\frac{12}{22}s)u_{i-1}^{j+1}+(1+\frac{51}{44}s)u_{i}^{j+1}+(\frac{2}{11}-\frac{12}{22}s)u_{i+1}^{j+1}-\frac{3}{88}su_{i+2}^{j+1}\\
&=\frac{3}{88}su_{i-2}^{j}+(\frac{2}{11}+\frac{12}{22}s)u_{i-1}^{j}+(1-\frac{51}{44}s)u_{i}^{j}+(\frac{2}{11}+\frac{12}{22}s)u_{i+1}^{j}+\frac{3}{88}su_{i+2}^{j}+\Delta t(\frac{2}{11}\varphi_{i-1}^{j}+\varphi_{i}^{j}+\frac{2}{11}\varphi_{i+1}^{j}),
\end{aligned}$$

where $s=\frac{\Delta t}{h^2},\ i=3,4,\cdots,M-1$.

According to Eq (2.5), at the boundary points x_1, x_2, x_3, x_4, x_5, and x_6, we have the following:

$$\begin{aligned}
&\frac{\partial u}{\partial t}|_{x=x_1}+\frac{137}{13}\frac{\partial u}{\partial t}|_{x=x_2}\\
&=u_1''+\frac{137}{13}u_2''+\varphi(u)|_{x=x_1}+\frac{137}{13}\varphi(u)|_{x=x_2}\\
&=\frac{1}{h^2}(\frac{1955}{156}u_1-\frac{4057}{156}u_2+\frac{1117}{78}u_3-\frac{55}{78}u_4-\frac{29}{156}u_5+\frac{7}{156}u_6)+\varphi(u)|_{x=x_1}+\frac{137}{13}\varphi(u)|_{x=x_2}.
\end{aligned}$$

Using the Crank-Nicolson scheme in time, we obtain the following:

$$\begin{aligned}
&\frac{u_1^{j+1}-u_1^{j}}{\Delta t}+\frac{137}{13}\frac{u_2^{j+1}-u_2^{j}}{\Delta t}\\
&=\frac{1}{2h^2}[(\frac{1955}{156}u_1^{j+1}-\frac{4057}{156}u_2^{j+1}+\frac{1117}{78}u_3^{j+1}-\frac{55}{78}u_4^{j+1}-\frac{29}{156}u_5^{j+1}+\frac{7}{156}u_6^{j+1})\\
&\quad+(\frac{1955}{156}u_1^{j}-\frac{4057}{156}u_2^{j}+\frac{1117}{78}u_3^{j}-\frac{55}{78}u_4^{j}-\frac{29}{156}u_5^{j}+\frac{7}{156}u_6^{j})]+\varphi_1^j+\frac{137}{13}\varphi_2^j.
\end{aligned}$$

After simplification, the difference scheme at the boundary is as follows:

$$\begin{aligned}
&(1-\frac{1955}{312}s)u_1^{j+1}+(\frac{137}{13}+\frac{4057}{312}s)u_2^{j+1}-\frac{1117}{156}su_3^{j+1}+\frac{55}{156}su_4^{j+1}+\frac{29}{312}su_5^{j+1}-\frac{7}{312}su_6^{j+1}\\
&=(1+\frac{1955}{312}s)u_1^{j}+(\frac{137}{13}-\frac{4057}{312}s)u_2^{j}+\frac{1117}{156}su_3^{j}-\frac{55}{156}su_4^{j}-\frac{29}{312}su_5^{j}+\frac{7}{312}su_6^{j}+\Delta t(\varphi_1^j+\frac{137}{13}\varphi_2^j).
\end{aligned}$$

Applying the same procedure at the boundary points x_{M-4}, x_{M-3}, x_{M-2}, x_{M-1}, x_M, and x_{M+1}, the difference schemes are summarized as follows:

$$\begin{aligned}
&(1-\frac{1955}{312}s)u_1^{j+1}+(\frac{137}{13}+\frac{4057}{312}s)u_2^{j+1}-\frac{1117}{156}su_3^{j+1}+\frac{55}{156}su_4^{j+1}+\frac{29}{312}su_5^{j+1}-\frac{7}{312}su_6^{j+1}\\
&=(1+\frac{1955}{312}s)u_1^{j}+(\frac{137}{13}-\frac{4057}{312}s)u_2^{j}+\frac{1117}{156}su_3^{j}-\frac{55}{156}su_4^{j}-\frac{29}{312}su_5^{j}+\frac{7}{312}su_6^{j}+\Delta t(\varphi_1^j+\frac{137}{13}\varphi_2^j),
\end{aligned}\tag{3.1}$$

$$
\begin{aligned}
&-\frac{3}{88}su_{i-2}^{j+1}+(\frac{2}{11}-\frac{12}{22}s)u_{i-1}^{j+1}+(1+\frac{51}{44}s)u_i^{j+1}+(\frac{2}{11}-\frac{12}{22}s)u_{i+1}^{j+1}-\frac{3}{88}su_{i+2}^{j+1}\\
&=\frac{3}{88}su_{i-2}^{j}+(\frac{2}{11}+\frac{12}{22}s)u_{i-1}^{j}+(1-\frac{51}{44}s)u_i^{j}+(\frac{2}{11}+\frac{12}{22}s)u_{i+1}^{j}+\frac{3}{88}su_{i+2}^{j} \qquad (3.2)\\
&+\Delta t(\frac{2}{11}\varphi_{i-1}^{j}+\varphi_i^{j}+\frac{2}{11}\varphi_{i+1}^{j}),\quad i=3,4,\ldots,M-1,
\end{aligned}
$$

$$
\begin{aligned}
&(1-\frac{1955}{312}s)u_{M+1}^{j+1}+(\frac{137}{13}+\frac{4057}{312}s)u_M^{j+1}-\frac{1117}{156}su_{M-1}^{j+1}+\frac{55}{156}su_{M-2}^{j+1}+\frac{29}{312}su_{M-3}^{j+1}-\frac{7}{312}su_{M-4}^{j+1}\\
&=(1+\frac{1955}{312}s)u_{M+1}^{j}+(\frac{137}{13}-\frac{4057}{312}s)u_M^{j}+\frac{1117}{156}su_{M-1}^{j}-\frac{55}{156}su_{M-2}^{j}-\frac{29}{312}su_{M-3}^{j}+\frac{7}{312}su_{M-4}^{j} \qquad (3.3)\\
&+\Delta t(\varphi_{M+1}^{j}+\frac{137}{13}\varphi_M^{j}).
\end{aligned}
$$

Furthermore, it can be written in matrix form as follows:

$$Au^{j+1}=Bu^{j}+C\varphi^{j}+D^{j},$$

where

$$\varphi^{j}=(\varphi_2^{j},\varphi_3^{j},\cdots,\varphi_M^{j})^{T},\quad u^{j}=(u_2^{j},u_3^{j},\cdots,u_M^{j})^{T},$$

$$
A=\begin{pmatrix}
\frac{137}{13}+\frac{4057}{312}s & -\frac{1117}{156}s & \frac{55}{156}s & \frac{29}{312}s & -\frac{7}{312}s & & \\
\frac{2}{11}-\frac{12}{22}s & 1+\frac{51}{44}s & \frac{2}{11}-\frac{12}{22}s & -\frac{3}{88}s & 0 & & \\
-\frac{3}{88}s & \frac{2}{11}-\frac{12}{22}s & 1+\frac{51}{44}s & \frac{2}{11}-\frac{12}{22}s & -\frac{3}{88}s & & \\
& \ddots & \ddots & \ddots & \ddots & \ddots & \\
& & -\frac{3}{88}s & \frac{2}{11}-\frac{12}{22}s & 1+\frac{51}{44}s & \frac{2}{11}-\frac{12}{22}s & -\frac{3}{88}s\\
& & 0 & -\frac{3}{88}s & \frac{2}{11}-\frac{12}{22}s & 1+\frac{51}{44}s & \frac{2}{11}-\frac{12}{22}s\\
& & -\frac{7}{312}s & \frac{29}{312}s & \frac{55}{156}s & -\frac{1117}{156}s & \frac{137}{13}+\frac{4057}{312}s
\end{pmatrix},
$$

$$
B=\begin{pmatrix}
\frac{137}{13}-\frac{4057}{312}s & \frac{1117}{156}s & -\frac{55}{156}s & -\frac{29}{312}s & \frac{7}{312}s & & \\
\frac{2}{11}+\frac{12}{22}s & 1-\frac{51}{44}s & \frac{2}{11}+\frac{12}{22}s & \frac{3}{88}s & 0 & & \\
\frac{3}{88}s & \frac{2}{11}+\frac{12}{22}s & 1-\frac{51}{44}s & \frac{2}{11}+\frac{12}{22}s & \frac{3}{88}s & & \\
& \ddots & \ddots & \ddots & \ddots & \ddots & \\
& & \frac{3}{88}s & \frac{2}{11}+\frac{12}{22}s & 1-\frac{51}{44}s & \frac{2}{11}+\frac{12}{22}s & \frac{3}{88}s\\
& & 0 & \frac{3}{88}s & \frac{2}{11}+\frac{12}{22}s & 1-\frac{51}{44}s & \frac{2}{11}+\frac{12}{22}s\\
& & \frac{7}{312}s & -\frac{29}{312}s & -\frac{55}{156}s & \frac{1117}{156}s & \frac{137}{13}-\frac{4057}{312}s
\end{pmatrix},
$$

$$C = \Delta t \begin{pmatrix} \frac{137}{13} & 0 & 0 & & \\ \frac{2}{11} & 1 & \frac{2}{11} & & \\ & \ddots & \ddots & \ddots & \\ & & \frac{2}{11} & 1 & \frac{2}{11} \\ & & 0 & 0 & \frac{137}{13} \end{pmatrix}, \; D^j = \begin{pmatrix} -(1-\frac{1955}{312}s)u_1^{j+1} + (1+\frac{1955}{312}s)u_1^j + k\varphi_1^j \\ \frac{3}{88}su_1^{j+1} + \frac{3}{88}su_1^j \\ 0 \\ \vdots \\ 0 \\ \frac{3}{88}su_{M+1}^{j+1} + \frac{3}{88}su_{M+1}^j \\ -(1-\frac{1955}{312}s)u_{M+1}^{j+1} + (1+\frac{1955}{312}s)u_{M+1}^j + k\varphi_{M+1}^j \end{pmatrix}.$$

By solving the above equation, the value at each time step can be obtained.

4. Stability and convergence analysis

In this section, we study the stability and convergence of numerical solutions to the FHN equation using the difference schemes (3.1)–(3.3) under the boundary value problems (1.2) and (1.3). To facilitate the error analysis, we rewrite our difference schemes in terms of derivative approximations.

According to the previous derivation, and by taking $c = \beta = 0$, the difference scheme (3.2) can also be written as follows:

$$\begin{aligned} &\alpha\frac{u_{i-1}^{j+1}-u_{i-1}^j}{k} + \frac{u_i^{j+1}-u_i^j}{k} + \alpha\frac{u_{i+1}^{j+1}-u_{i+1}^j}{k} \\ &= \frac{1}{2}\left[a\left(\frac{u_{i-1}^{j+1}-2u_i^{j+1}+u_{i+1}^{j+1}}{h^2} + \frac{u_{i-1}^j-2u_i^j+u_{i+1}^j}{h^2}\right) + b\left(\frac{u_{i-2}^{j+1}-2u_i^{j+1}+u_{i+2}^{j+1}}{4h^2} + \frac{u_{i-2}^j-2u_i^j+u_{i+2}^j}{4h^2}\right)\right] \\ &\quad + \alpha\varphi_{i-1}^j + \varphi_i^j + \alpha\varphi_{i+1}^j, \quad 3 \le i \le M-1. \end{aligned} \tag{4.1}$$

Looking back at Eq (2.2), the coefficients a, b, and α satisfy the following relationship:

$$\begin{cases} a + b = 1 + 2\alpha, \\ a + 4b = 12\alpha, \\ a + 16b = 30\alpha. \end{cases} \tag{4.2}$$

4.1. Stability analysis

We define some operators and inner products as follows:

$$\delta_{xx}^{(1)}u_i = \frac{u_{i-1}-2u_i+u_{i+1}}{h^2}, \quad \delta_{xx}^{(2)}u_i = \frac{u_{i-2}-2u_i+u_{i+2}}{4h^2},$$

$$\mathcal{L}v = a\delta_{xx}^{(1)}v + b\delta_{xx}^{(2)}v, \quad (\mathcal{M}v)_i = \alpha v_{i-1} + v_i + \alpha v_{i+1},$$

$$\langle v, w\rangle = h\sum_{i=3}^{M-1} v_i w_i, \quad \|v\|^2 = \langle v, v\rangle, \quad \langle v, w\rangle_{\mathcal{M}} = \langle \mathcal{M}v, w\rangle, \quad \|v\|_{\mathcal{M}}^2 = \langle v, v\rangle_{\mathcal{M}}.$$

Thus, the operator form of (4.1) is as follows:

$$\frac{\mathcal{M}u^{j+1} - \mathcal{M}u^j}{k} = \frac{1}{2}\left(\mathcal{L}u^{j+1} + \mathcal{L}u^j\right) + \mathcal{M}\varphi^j \quad (i = 3, \cdots, M-1). \tag{4.3}$$

To prove the stability of this method, we need to use the following lemma.

Lemma 4.1. *If $0 < \alpha < \frac{1}{2}$, then $\mathcal{M}$ is symmetric and positive definite; additionally,*

$$c_0 \|v\|^2 \le \|v\|_{\mathcal{M}}^2 \le c_1 \|v\|^2, \quad c_0 = 1 - 2\alpha, c_1 = 1 + 2\alpha.$$

Proof. Expanding

$$\|v\|_{\mathcal{M}}^2 = h \sum_{i=3}^{M-1} (v_i^2 + \alpha v_{i-1} v_i + \alpha v_i v_{i+1}), \tag{4.4}$$

from $|ab| \le \frac{1}{2}(a^2 + b^2)$, we obtain

$$-\frac{1}{2}(v_i^2 + v_{i+1}^2) \le v_i v_{i+1} \le \frac{1}{2}(v_i^2 + v_{i+1}^2).$$

Summing Eq (4.4) for $i = 3, \cdots, M-2$, we obtain the following:

$$\sum_{i=3}^{M-2} v_i v_{i+1} \ge -\frac{1}{2}\sum_{i=3}^{M-2}\left(v_i^2 + v_{i+1}^2\right) = -\frac{1}{2}v_3^2 - \sum_{i=4}^{M-2} v_i^2 - \frac{1}{2}v_{M-1}^2 \ge -\sum_{i=3}^{M-1} v_i^2,$$

$$\sum_{i=3}^{M-2} v_i v_{i+1} \le \tfrac{1}{2}\sum_{i=3}^{M-2}(v_i^2 + v_{i+1}^2) = \tfrac{1}{2}v_3^2 + \sum_{i=4}^{M-2} v_i^2 + \tfrac{1}{2}v_{M-1}^2 \le \sum_{i=3}^{M-1} v_i^2.$$

Thus,

$$-\sum_{i=3}^{M-1} v_i^2 \le \sum_{i=3}^{M-2} v_i v_{i+1} \le \sum_{i=3}^{M-1} v_i^2. \tag{4.5}$$

Substituting (4.5) into (4.4), since $\alpha > 0$ and $h > 0$, we obtain the upper and lower bounds as follows:

$$\|v\|_{\mathcal{M}}^2 \ge h\sum v_i^2 + 2\alpha\left(-h\sum v_i^2\right) = (1-2\alpha)h\sum v_i^2 = (1-2\alpha)\|v\|^2 = c_0\|v\|^2,$$

$$\|v\|_{\mathcal{M}}^2 \le h\sum v_i^2 + 2\alpha\left(h\sum v_i^2\right) = (1+2\alpha)h\sum v_i^2 = (1+2\alpha)\|v\|^2 = c_1\|v\|^2.$$

Furthermore, since $\alpha < \frac{1}{2}$, we have $c_0 = 1 - 2\alpha > 0$; therefore,

$$\|v\|_{\mathcal{M}}^2 \ge c_0\|v\|^2 > 0.$$

Thus, $\mathcal{M}$ is positive definite, and symmetry is obvious from the definition; thus, $\mathcal{M}$ is symmetric and positive definite. □

Lemma 4.2. *Suppose that the sequence extends to zero at the boundary; then,*

$$\left\langle v, \delta_{xx}^{(1)} v\right\rangle = -\|\mathcal{D}_1 v\|^2, \quad \left\langle v, \tfrac{1}{4}\delta_{xx}^{(2)} v\right\rangle = -\|\mathcal{D}_2 v\|^2,$$

where $(\mathcal{D}_1 v)_i = (v_{i+1} - v_i)/h$ and $(\mathcal{D}_2 v)_i = (v_{i+1} - v_{i-1})/(2h)$. Therefore,

$$\langle v, \mathcal{L}v\rangle = -a\|\mathcal{D}_1 v\|^2 - b\|\mathcal{D}_2 v\|^2 \le 0.$$

Proof. For the first equation, since it extends to zero at the boundary, we have the following:

$$\sum v_i(v_{i-1} - 2v_i + v_{i+1}) = \sum [(v_i - v_{i-1})v_{i-1} - (v_{i+1} - v_i)v_i] = -\sum (v_{i+1} - v_i)^2 .$$

We multiply both sides by $\frac{1}{h^2}$ to obtain

$$\left\langle v, \delta_{xx}^{(1)} v \right\rangle = \frac{1}{h^2} \sum v_i(v_{i-1} - 2v_i + v_{i+1}) = -\frac{1}{h^2} \sum (v_{i+1} - v_i)^2 = -\|D_1 v\|^2 ;$$

thus, the first equation is proven.

For the second equation, let $A_i = \frac{v_{i+1} - v_{i-1}}{2h}$; then,

$$\frac{A_{i+1} - A_{i-1}}{2h} = \frac{v_{i+2} - 2v_i + v_{i-2}}{4h} = \delta_{xx}^{(2)} v_i.$$

Thus,

$$\sum hv_i \cdot \tfrac{1}{4}\delta_{xx}^{(2)} v_i = \sum \tfrac{h}{4} v_i \tfrac{A_{i+1} - A_{i-1}}{2h} = \tfrac{1}{2} \sum v_i(A_{i+1} - A_{i-1}) = -\tfrac{1}{2} \sum A_i(v_{i+1} - v_{i-1}) = -\sum hA_i^2,$$

that is,

$$\left\langle v, \tfrac{1}{4}\delta_{xx}^{(2)} v \right\rangle = -\|\mathcal{D}_2 v\|^2 .$$

The second equation is proven, and Lemma 4.2 is complete. □

Next, define the linear extension of each time layer based on the boundary conditions $u(p, t) = f_1(t)$ and $u(q, t) = f_2(t)$ as follows:

$$g(x, t_j) = f_1(t_j) + \frac{x - p}{q - p}(f_2(t_j) - f_1(t_j)).$$

It can also be written as follows:

$$g_i^j = (1 - \lambda_i) f_1^j + \lambda_i f_2^j,$$

where $\lambda_i = \frac{x_i - p}{q - p} = \frac{i-1}{M}$. Thus,

$$g_1^j = f_1^j, \quad g_{M+1}^j = f_2^j,$$

and it is clear that g^j is linear with respect to x. Thus,

$$\delta_{xx}^{(1)} g^j \equiv \delta_{xx}^{(2)} g^j \equiv \mathcal{L} g^j \equiv 0.$$

Let $v^j = u^j - g^j$; substitute $u^j = v^j + g^j$ into (4.3), use $\mathcal{L} g^j = 0$, and organize to obtain the internal equation with zero boundary as follows:

$$\frac{\mathcal{M} v^{j+1} - \mathcal{M} v^j}{k} = \frac{1}{2}\left(\mathcal{L} u^{j+1} + \mathcal{L} u^j\right) + \mathcal{M}\varphi(v^j + g^j) + \frac{\mathcal{M}(g^{j+1} - g^j)}{k}. \tag{4.6}$$

Denote

$$R^j = \frac{\mathcal{M}(g^{j+1} - g^j)}{k},$$

where

$$(R^j)_i = \alpha \delta_t g_{i-1}^j + \delta_t g_i^j + \alpha \delta_t g_{i+1}^j, \quad \delta_t g_i^j = \frac{g_i^{j+1} - g_i^j}{k} = (1 - \lambda_t)\delta_t f_1^j + \lambda_t \delta_t f_2^j,$$

$$\delta_t f_1^j = \frac{f_1(t_{j+1}) - f_1(t_{j+1})}{k}, \quad \delta_t f_2^j = \frac{f_2(t_{j+1}) - f_2(t_{j+1})}{k}.$$

Note that

$$\alpha(1-\lambda_{i-1}) + (1-\lambda_i) + \alpha(1-\lambda_{i+1}) + (\alpha\lambda_{i-1} + \lambda_i + \alpha\lambda_{i+1}) = 1 + 2\alpha.$$

We obtain a pointwise estimate as follows:

$$\left|(R^j)_i\right| \le (1+2\alpha)\max\left\{\left|\delta_t f_1^j\right|, \left|\delta_t f_2^j\right|\right\}.$$

Taking the inner product of both sides of (4.6) with $v^{j+1} + v^j$, and setting $w^{j+\frac{1}{2}} = \frac{1}{2}(v^{j+1} + v^j)$, then by the symmetry of $\mathcal{M}$ in Lemma 4.1 together with Lemma 4.2, we obtain the following:

$$\frac{\left\|v^{j+1}\right\|_{\mathcal{M}}^2 - \left\|v^j\right\|_{\mathcal{M}}^2}{k} = \frac{1}{2}\left\langle \mathcal{L}w^{j+\frac{1}{2}}, w^{j+\frac{1}{2}}\right\rangle + \left\langle \mathcal{M}\varphi(v^j + g^j), v^{j+1} + v^j\right\rangle + \left\langle R^j, v^{j+1} + v^j\right\rangle.$$

Moreover, the diffusion term satisfies the following:

$$\left\langle \mathcal{L}w^{j+\frac{1}{2}}, w^{j+\frac{1}{2}}\right\rangle = -a\left\|\mathcal{D}_1 w^{j+\frac{1}{2}}\right\|^2 - b\left\|\mathcal{D}_2 w^{j+\frac{1}{2}}\right\|^2 \le 0.$$

Thus,

$$\frac{\left\|v^{j+1}\right\|_M^2 - \left\|v^j\right\|_M^2}{k} \le \left\langle \mathcal{M}\varphi(v^j + g^j), v^{j+1} + v^j\right\rangle + \left\langle R^j, v^{j+1} + v^j\right\rangle. \tag{4.7}$$

Next, we decompose the nonlinear term into the Lipschitz part with respect to v and the pure data part as follows:

$$\varphi(v^j + g^j) = \left[\varphi(v^j + g^j) - \varphi(g^j)\right] + \varphi(g^j). \tag{4.8}$$

Denote

$$N^j = \varphi(v^j + g^j) - \varphi(g^j), \quad G^j = \varphi(g^j).$$

Let the amplitude upper bound be $K > 0$, which satisfies

$$\left|v_i^j + g_i^j\right| \le K, \quad \forall\, i, j \le n,$$

and define

$$L_K = \max_{|s|\le K}\left|\varphi'(s)\right|, \quad \phi_K = \max_{|s|\le K}\left|\varphi(s)\right|.$$

By the mean value theorem and $\varphi \in \mathbb{C}^1$, we obtain $\left|N_i^j\right| \le L_K\left|v_i^j\right|$. Combining this with Lemma 4.1, we have the following:

$$\left\|N^j\right\| \le L_K\left\|v^j\right\| \le \sqrt{\tfrac{1}{c_0}}L_K\left\|v^j\right\|_M. \tag{4.9}$$

Since $G^j = \varphi(g^j)$ is completely determined by the boundary data, it follows that

$$\left\|G^j\right\| \le \sqrt{q-p}\phi_K, \quad \left\|\mathcal{M}G^j\right\| \le (1+2\alpha)\sqrt{q-p}\phi_K.$$

Substituting (4.8) into (4.7), we obtain the following:

$$\frac{\left\|v^{j+1}\right\|_M^2 - \left\|v^j\right\|_M^2}{k} \le \left\langle \mathcal{M}N^j, v^{j+1} + v^j\right\rangle + \left\langle \mathcal{M}G^j, v^{j+1} + v^j\right\rangle + \left\langle R^j, v^{j+1} + v^j\right\rangle. \tag{4.10}$$

(i) For the first term on the right-hand side of the inequality, by the Cauchy-Schwarz inequality and (4.9), we have the following:

$$\left\langle MN^j, v^{j+1} + v^j \right\rangle \leq \left\|N^j\right\|_M \left\|v^{j+1} + v^j\right\|_M \leq \sqrt{\tfrac{c_1}{c_0}} L_K \left\|v^j\right\|_M \left(\left\|v^{j+1}\right\|_M + \left\|v^j\right\|_M\right).$$

Using $2ab \leq a^2 + b^2$, we have the following:

$$\left\|v^j\right\|_{\mathcal{M}} \left(\left\|v^{j+1}\right\|_{\mathcal{M}} + \left\|v^j\right\|_{\mathcal{M}}\right) \leq \frac{1}{2}\left(\left\|v^{j+1}\right\|_{\mathcal{M}}^2 + 3\left\|v^j\right\|_{\mathcal{M}}^2\right).$$

Let $\gamma = \sqrt{\frac{c_1}{c_0}} L_K$; then, we have the following:

$$\left\langle \mathcal{M}N^j, v^{j+1} + v^j \right\rangle \leq \frac{\gamma}{2}\left(\left\|v^{j+1}\right\|_{\mathcal{M}}^2 + 3\left\|v^j\right\|_{\mathcal{M}}^2\right). \tag{4.11}$$

(ii) For the second and third terms on the right-hand side of the inequality, by the Cauchy-Schwarz inequality and Lemma 4.1, we have the following:

$$\left\langle \mathcal{M}G^j, v^{j+1} + v^j \right\rangle \leq \left\|\mathcal{M}G^j\right\| \left\|v^{j+1} + v^j\right\| \leq \sqrt{\tfrac{2}{c_0}} \left\|\mathcal{M}G^j\right\| \max\left\{\left\|v^{j+1}\right\|_{\mathcal{M}}, \left\|v^j\right\|_{\mathcal{M}}\right\},$$

$$\left\langle R^j, v^{j+1} + v^j \right\rangle \leq \left\|R^j\right\| \left\|v^{j+1} + v^j\right\| \leq \sqrt{\tfrac{2}{c_0}} \left\|R^j\right\| \max\left\{\left\|v^{j+1}\right\|_M, \left\|v^j\right\|_M\right\}.$$

Applying $2ab \leq \varepsilon a^2 + \varepsilon^{-1} b^2$, $\forall \varepsilon \in (0, 1]$ to the above two formulas, we obtain the following:

$$\left\langle \mathcal{M}G^j, v^{j+1} + v^j \right\rangle + \left\langle R^j, v^{j+1} + v^j \right\rangle \leq \frac{\varepsilon}{2}\left(\left\|v^{j+1}\right\|_M^2 + \left\|v^j\right\|_M^2\right) + \frac{1}{\varepsilon}\frac{2}{c_0}\left(\left\|\mathcal{M}G^j\right\|^2 + \left\|R^j\right\|^2\right). \tag{4.12}$$

Substituting (4.11) and (4.12) into (4.10), we obtain the following:

$$\frac{\left\|v^{j+1}\right\|_{\mathcal{M}}^2 - \left\|v^j\right\|_{\mathcal{M}}^2}{k} \leq \frac{\gamma}{2}\left(\left\|v^{j+1}\right\|_{\mathcal{M}}^2 + 3\left\|v^j\right\|_{\mathcal{M}}^2\right) + \frac{\varepsilon}{2}\left(\left\|v^{j+1}\right\|_{\mathcal{M}}^2 + \left\|v^j\right\|_{\mathcal{M}}^2\right) + \frac{1}{\varepsilon}\frac{2}{c_0}\left(\left\|\mathcal{M}G^j\right\|^2 + \left\|R^j\right\|^2\right).$$

After simplification, we obtain the following:

$$\left(1 - \frac{k}{2}(\gamma + \varepsilon)\right)\left\|v^{j+1}\right\|_M^2 \leq \left(1 + k\left(\tfrac{3}{2}\gamma + \tfrac{1}{2}\varepsilon\right)\right)\left\|v^j\right\|_M^2 + k\frac{1}{\varepsilon}\frac{2}{c_0}\left(\left\|\mathcal{M}G^j\right\|^2 + \left\|R^j\right\|^2\right). \tag{4.13}$$

For $\forall \varepsilon \in (0, 1]$, if

$$k < \frac{2}{\gamma + \varepsilon},$$

then the coefficient on the left-hand side of (25) is positive, and hence it can be written as

$$\left\|v^{j+1}\right\|_{\mathcal{M}}^2 \leq \frac{1 + k\left(\frac{3}{2}\gamma + \frac{1}{2}\varepsilon\right)}{1 - \frac{k}{2}(\gamma + \varepsilon)}\left\|v^j\right\|_{\mathcal{M}}^2 + k\frac{1}{\varepsilon}\frac{2}{c_0}\frac{1}{1 - \frac{k}{2}(\gamma + \varepsilon)}\left(\left\|\mathcal{M}G^j\right\|^2 + \left\|R^j\right\|^2\right).$$

Denote

$$E^j = \left\|v^j\right\|_{\mathcal{M}}^2, \quad \rho_\varepsilon(k) = \frac{1 + k(\frac{3}{2}\gamma + \frac{1}{2}\varepsilon)}{1 - \frac{k}{2}(\gamma + \varepsilon)}, \quad C_\varepsilon = \frac{1}{\varepsilon}\frac{2}{c_0}\frac{1}{1 - \frac{k}{2}(\gamma + \varepsilon)}.$$

Then, the above expression can also be written as follows:

$$E^{j+1} \leq \rho_\varepsilon(k)E^j + kC_\varepsilon\left(\left\|\mathcal{M}G^j\right\|^2 + \left\|R^j\right\|^2\right).$$

For $\forall n \leq N$, iterating for $j = 1, \cdots, n$, we obtain the discrete Grönwall-type estimate as follows:

$$E^n \leq \rho_\varepsilon(k)^n E^0 + \sum_{j=1}^{n} k\rho_\varepsilon(k)^{n-j}C_\varepsilon\left(\left\|\mathcal{M}G^j\right\|^2 + \left\|R^j\right\|^2\right).$$

By Grönwall's lemma, the solution is exponentially bounded.

Therefore, as long as the time step satisfies $k < \frac{2}{\gamma+\varepsilon}$, the energy of the numerical solution remains bounded, which proves the stability of the difference scheme (3.2). Similarly, the stability of the schemes (3.1) and (3.3) can be established.

4.2. Convergence analysis

Recalling (4.1),

$$\begin{aligned}
&\alpha\frac{u_{i-1}^{j+1} - u_{i-1}^{j}}{k} + \frac{u_i^{j+1} - u_i^j}{k} + \alpha\frac{u_{i+1}^{j+1} - u_{i+1}^{j}}{k} \\
&= \frac{1}{2}\left[a\left(\frac{u_{i-1}^{j+1} - 2u_i^{j+1} + u_{i+1}^{j+1}}{h^2} + \frac{u_{i-1}^{j} - 2u_i^{j} + u_{i+1}^{j}}{h^2}\right) + b\left(\frac{u_{i-2}^{j+1} - 2u_i^{j+1} + u_{i+2}^{j+1}}{4h^2} + \frac{u_{i-2}^{j} - 2u_i^{j} + u_{i+2}^{j}}{4h^2}\right)\right] \\
&\quad + \alpha\varphi_{i-1}^j + \varphi_i^j + \alpha\varphi_{i+1}^j, \quad 3 \leq i \leq M-1.
\end{aligned}$$

We use the following notation:

$$H_1^j = \frac{u_{i-1}^j - 2u_i^j + u_{i+1}^j}{h^2}, \quad H_2^j = \frac{u_{i-2}^j - 2u_i^j + u_{i+2}^j}{4h^2},$$

$$\omega_{-1} = \alpha,\ \omega_0 = 1,\ \omega_1 = \alpha,\ m \in \{-1, 0, 1\},\ S_n = \sum_m m^n\omega_m.$$

Then, we have the following:

$$S_0 = \sum_m \omega_m = 1 + 2\alpha, \quad S_2 = \sum_m m^2\omega_m = 2\alpha, \quad S_4 = \sum_m m^4\omega_m = 2\alpha, \quad S_1 = S_5 = 0.$$

Therefore, Eq (4.1) may be represented as follows:

$$\frac{1}{k}\sum_m \omega_m\left(u(x_{i+m}, t_{j+1}) - u(x_{i+m}, t_j)\right) = \frac{1}{2}\left[a\left(H_1^{j+1} + H_1^j\right) + b\left(H_2^{j+1} + H_2^j\right)\right] + \sum_m \omega_m\varphi_{i+m}^j.$$

For the left-hand side of the equation, by performing a Taylor expansion in time t_j, we obtain the following:

$$u(x_{i+m}, t_{j+1}) - u(x_{i+m}, t_j) = ku_t(x_{i+m}, t_j) + \frac{k^2}{2}u_{tt}(x_{i+m}, t_j) + O(k^3).$$

Furthermore, expanding each time derivative in space with respect to x_i, we obtain the following:

$$u_t(x_{i+m}, t_j) = u_t + mhu_{xt} + \frac{m^2h^2}{2}u_{xxt} + \frac{m^3h^3}{6}u_{xxxt} + \frac{m^4h^4}{24}u_{xxxxt} + O(h^5),$$

$$u_{tt}(x_{i+m}, t_j) = u_{tt} + mhu_{xtt} + +\frac{m^2h^2}{2}u_{xxtt} + \frac{m^3h^3}{6}u_{xxxtt} + \frac{m^4h^4}{24}u_{xxxxtt} + O(h^5).$$

Thus,

$$\begin{aligned}
\text{LHS} &= \frac{1}{k}\sum_m \omega_m \Big(u(x_{i+m}, t_{j+1}) - u(x_{i+m}, t_j)\Big) \\
&= \frac{1}{k}\sum_m \omega_m \bigg(ku_t(x_{i+m}, t_j) + \frac{k^2}{2}u_{tt}(x_{i+m}, t_j) + O(k^3)\bigg) \\
&= \sum_m \omega_m \bigg(u_t(x_{i+m}, t_j) + \frac{k}{2}u_{tt}(x_{i+m}, t_j) + O(k^2)\bigg) \\
&= \sum_m \omega_m \bigg[\bigg(u_t + mhu_{xt} + \frac{m^2h^2}{2}u_{xxt} + \frac{m^3h^3}{6}u_{xxxt} + \frac{m^4h^4}{24}u_{xxxxt} + O(h^5)\bigg) \\
&\quad + \frac{k}{2}\bigg(u_{tt} + mhu_{xtt} + \frac{m^2h^2}{2}u_{xxtt} + \frac{m^3h^3}{6}u_{xxxtt} + \frac{m^4h^4}{24}u_{xxxxtt} + O(h^5)\bigg) + O(k^2)\bigg] \\
&= \sum_m \omega_m u_t + \frac{h^2}{2}\sum_m m^2\omega_m u_{xxt} + \frac{h^4}{24}\sum_m m^4\omega_m u_{xxxxt} + \frac{k}{2}\sum_m \omega_m u_{tt} + O(k^2, kh^2, h^6) \\
&= S_0u_t + \frac{k}{2}S_0u_{tt} + \frac{h^2}{2}S_2u_{xxt} + \frac{h^4}{24}S_4u_{xxxxt} + O(k^2, kh^2, h^6).
\end{aligned}$$

For the right-hand side of the equation, by performing a Taylor expansion of H_1^j, H_2^j, H_1^{j+1}, and H_2^{j+1} in (x_i, t_j), and expanding φ_{i+m}^j in x_i, we obtain the following:

$$\begin{aligned}
\text{RHS} &= \frac{1}{2}\Big(aH_1^j + bH_2^j + aH_1^{j+1} + bH_2^{j+1}\Big) + \sum_m \omega_m\varphi_{i+m}^j \\
&= \frac{1}{2}\bigg[a\bigg(u_{xx} + \frac{h^2}{12}u_{xxxx} + \frac{h^4}{360}u^{(6)} + O(h^6)\bigg) + b\bigg(u_{xx} + \frac{h^2}{3}u_{xxxx} + \frac{2h^4}{45}u^{(6)} + O(h^6)\bigg) \\
&\quad + a\bigg(u_{xx}(x_i, t_{j+1}) + \frac{h^2}{12}u_{xxxx}(x_i, t_{j+1}) + \frac{h^4}{360}u^{(6)}(x_i, t_{j+1}) + O(h^6)\bigg) \\
&\quad + b\bigg(u_{xx}(x_i, t_{j+1}) + \frac{h^2}{3}u_{xxxx}(x_i, t_{j+1}) + \frac{2h^4}{45}u^{(6)}(x_i, t_{j+1}) + O(h^6)\bigg)\bigg] \\
&\quad + \sum_m \omega_m \bigg(\varphi + mh\varphi_x + \frac{m^2h^2}{2}\varphi_{xx} + \frac{m^3h^3}{6}\varphi_{xxx} + \frac{m^4h^4}{24}\varphi_{xxxx} + O(h^5)\bigg) \\
&= (a+b)u_{xx} + \frac{k}{2}(a+b)u_{xxt} + h^2(\frac{a}{12} + \frac{b}{3})u_{xxxx} + \frac{kh^2}{2}(\frac{a}{12} + \frac{b}{3})u_{xxxxt} + h^4(\frac{a}{360} + \frac{2b}{45})u^{(6)} \\
&\quad + \sum_m \omega_m\varphi + \frac{h^2}{2}\sum_m m^2\omega_m\varphi_{xx} + \frac{h^4}{24}\sum_m m^4\omega_m\varphi_{xxxx} + O(k^2, kh^2, h^6)
\end{aligned}$$

$$= (a+b)u_{xx} + \frac{k}{2}(a+b)u_{xxt} + h^2(\frac{a}{12} + \frac{b}{3})u_{xxxx} + \frac{kh^2}{2}(\frac{a}{12} + \frac{b}{3})u_{xxxxt} + h^4(\frac{a}{360} + \frac{2b}{45})u^{(6)}$$
$$+ S_0\varphi + \frac{h^2}{2}S_2\varphi_{xx} + \frac{h^4}{24}S_4\varphi_{xxxx} + O(k^2, kh^2, h^6).$$

Therefore,

$$\tau = LHS - RHS$$
$$= (S_0u_t - (a+b)u_{xx} - S_0\varphi) + \frac{k}{2}(S_0u_{tt} - (a+b)u_{xxt}) + \frac{h^2}{2}\left(S_2u_{xxt} - 2(\frac{a}{12} + \frac{b}{3})u_{xxxx} - S_2\varphi_{xx}\right)$$
$$+ \frac{h^4}{24}\left(S_4u_{xxxxt} - 24(\frac{a}{360} + \frac{2b}{45})u^{(6)} - S_4\varphi_{xxxx}\right) + O(k^2, kh^2, h^6).$$

According to (4.2), we have the following:

$$\begin{cases} a + b = 1 + 2\alpha = S_0, \\ \frac{1}{6}a + \frac{2}{3}b = 2\alpha = S_2, \\ \frac{1}{15}a + \frac{16}{15}b = 2\alpha = S_4. \end{cases}$$

Thus,

$$\tau = (S_0u_t - S_0u_{xx} - S_0\varphi) + \frac{k}{2}(S_0u_{tt} - S_0u_{xxt}) + \frac{h^2}{2}(S_2u_{xxt} - S_2u_{xxxx} - S_2\varphi_{xx})$$
$$+ \frac{h^4}{24}\left(S_4u_{xxxt} - S_4u^{(6)} - S_4\varphi_{xxxx}\right) + O(k^2, kh^2, h^6).$$

From (1.1), since $u_t - u_{xx} - \varphi = 0$, by differentiating both sides of the equation with respect to x or t, we obtain the following:

$$\begin{cases} u_{xt} - u_{xxx} + \varphi_x = 0, \\ u_{tt} - u_{xxt} = \varphi_t, \\ u_{xxt} - u_{xxxx} - \varphi_{xx} = 0, \\ u_{xxxxt} - u^{(6)} - \varphi_{xxxx} = 0. \end{cases}$$

Thus,

$$\tau = \frac{k}{2}S_0\varphi_t + O(k^2, kh^2, h^6).$$

This means that, as $h, k \to 0$, the truncation error $\tau \to 0$, which indicates that the difference scheme is consistent. Since we have already proven the stability earlier, it follows from the Lax equivalence theorem that our difference scheme is convergent.

Moreover, we also know that the truncation error of Eq (3.2) is $O(k + h^6)$. Similarly, the truncation errors of (3.1) and (3.3) are also $O(k + h^6)$. This result will be verified in the numerical experiments in the next section.

5. Numerical examples

The method is assessed in terms of the L_2 and L_∞ error norms and the order of convergence, which are defined as follows:

$$L_2 = \sqrt{\sum_{i=0}^{M}\sum_{j=0}^{N}\left(u(x_i,t_j)-u_{exa}(x_i,t_j)\right)^2},\quad L_\infty = \max_{0\le i\le M,0\le j\le N}\left|u(x_i,t_j)-u_{exa}(x_i,t_j)\right|,\quad rate = \frac{\log(E_1/E_2)}{\log(h_1/h_2)},$$

where $u_{exa}(x_i,t_j)$ represents the exact solution at $x = x_i$, $t = t_j$, and E_1, E_2 denote the corresponding L_∞ errors when the spatial step of the lattice is h_1, h_2, respectively.

We consider the FHN equation

$$\frac{\partial u}{\partial t} = \frac{\partial^2 u}{\partial x^2} + u(1-u)(u-\theta),\quad (x,t)\in[p,q]\times[0,T]$$

with the initial condition

$$u(x,0) = \frac{1}{2} + \frac{1}{2}\tanh\left(\frac{x}{2\sqrt{2}}\right),$$

and boundary conditions

$$u(p,t) = \frac{1}{2} + \frac{1}{2}\tanh\left[\frac{1}{2\sqrt{2}}(p+ct)\right],\quad u(q,t) = \frac{1}{2} + \frac{1}{2}\tanh\left[\frac{1}{2\sqrt{2}}(q+ct)\right],$$

respectively, where $c = \frac{1}{\sqrt{2}}(1-2\theta)$.

Thus, the exact solution of this equation is

$$u(x,t) = \frac{1}{2} + \frac{1}{2}\tanh\left[\frac{1}{2\sqrt{2}}(x+ct)\right].$$

In what follows, we apply the algorithm proposed in this paper to Eq (1.1) under two sets of initial data.

Case 1: Set the initial data $p = -10$, $q = 10$, $T = 1$, and $\theta = 0.5$, and the fixed time step $\Delta t = 10^{-2}$.

Table 1 shows the results of the comparison between the numerical solution and the exact solution at different spatial locations when the spatial step size h is taken as 0.5, 0.25 and 0.125. It can be seen that the error between the numerical solution and the analytical solution significantly decreases as the spatial step size decreases. Figure 1 shows the comparison between the three-dimensional images of the numerical solution and the exact solution when h is taken as 0.5 and 0.25. It can be seen that the numerical simulation results basically match with the exact solution image, which verifies the effectiveness of the algorithm.

Table 1. Comparison of numerical solutions and exact solutions for different spatial step sizes.

x	Numerical solutions			Exact solutions
	$h = 0.5$	$h = 0.25$	$h = 0.125$	
-8	0.003481327309947	0.003481327293309	0.003481327296985	0.003481327297065
-6	0.014166030241687	0.014166035788835	0.014166035875316	0.014166035876688
-4	0.055807233852591	0.055807219442184	0.055807219210866	0.055807219207170
-2	0.195570322854545	0.195570317536785	0.195570317493569	0.195570317493043
0	0.499999999999997	0.499999999999994	0.500000000000002	0.500000000000000
2	0.804429677145450	0.804429682463204	0.804429682506434	0.804429682506957
4	0.944192766147403	0.944192780557806	0.944192780789137	0.944192780792830
6	0.985833969758309	0.985833964211155	0.985833964124688	0.985833964123312
8	0.996518672690049	0.996518672706683	0.996518672703019	0.996518672702935

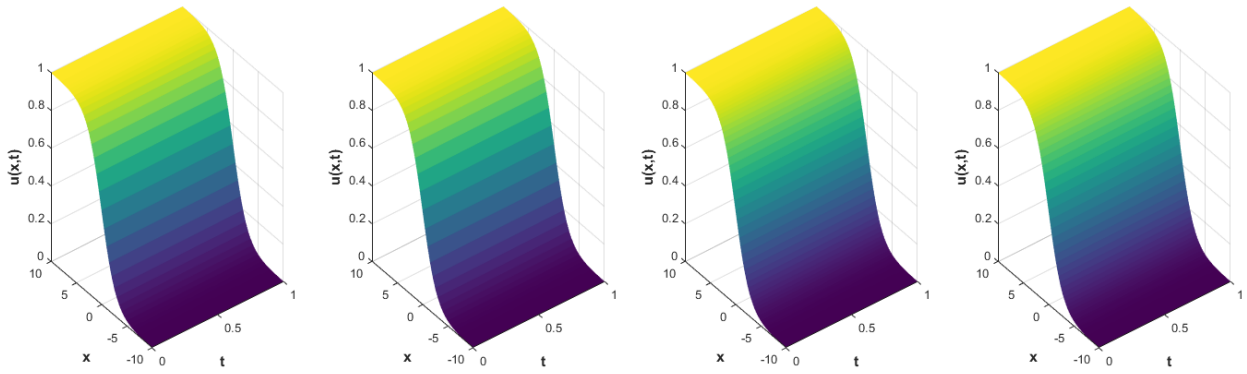

(a) Numerical, $h = 0.5$ **(b)** Exact, $h = 0.5$ **(c)** Numerical, $h = 0.25$ **(d)** Exact, $h = 0.25$

Figure 1. Comparison of numerical and exact solutions for different h.

Table 2 lists the comparison of the backward Euler method, the algorithm of the literature [17], and the algorithm of this paper for different spatial step sizes that correspond to the L_2 error, L_∞ error, and convergence order. From the data in the table, it can be seen that the numerical accuracy of the algorithm in this paper is superior. With the increase of the number of spatial discrete points, the error decreases, the convergence order is close to the sixth order, and the numerical solution shows good stability under different spatial resolutions. Figure 2 illustrates the errors at each discrete point at time t = 1 when the spatial space step h is taken as 1, 0.5, 0.25 and 0.125. As can be seen from Figure 2, the trend of the error images is similar at different spatial steps, and the order of magnitude of the error steadily decreases as h decreases, which proves that the method is stable and convergent.

Table 2. Comparison of the L_2 errors, L_∞ errors, and convergence order of different algorithms.

h	backward Euler method		the algorithm of the [17]		the algorithm in this paper	
	L_∞	order	L_∞	order	L_∞	order
1	1.5460×10^{-3}	–	1.1055×10^{-4}	–	1.5524×10^{-5}	–
0.5	4.0850×10^{-4}	1.9202	5.9802×10^{-6}	4.0859	2.1853×10^{-7}	6.1505
0.25	1.0197×10^{-4}	2.0021	3.6832×10^{-7}	4.0212	3.3936×10^{-9}	6.0089
0.125	5.5657×10^{-5}	1.9908	2.2936×10^{-8}	4.0053	5.3193×10^{-11}	5.9954
0.0625	6.4132×10^{-6}	2.0002	1.4366×10^{-9}	3.9968	8.4049×10^{-13}	5.9839

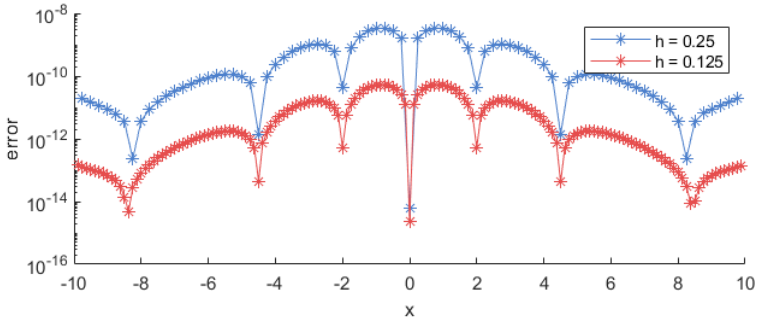

Figure 2. Numerical errors of discrete points with different M values at time t=1.

Case 2: Set the initial data $p = -5$, $q = 25$, $T = 0.5$, and $\theta = 0.5$, and the fixed time step $\Delta t = 10^{-2}$.

Table 3 shows the comparison results between the numerical solution and the analytical solution at different spatial locations when the spatial step size h is set to 0.5, 0.25, and 0.125. It can be seen that as the spatial step size decreases, the error between the numerical solution and the analytical solution significantly decreases. Figure 3 shows the comparison of the three-dimensional images of the numerical solution and the analytical solution when the spatial step size h is set to 0.5 and 0.25. It can be seen that the numerical simulation results are basically consistent with the analytical solution images.

Table 4 lists the comparison of the L_2 error, L_∞ error, and convergence order of the three algorithms under different spatial step sizes. From the data in the table, it can be seen that the numerical accuracy of the algorithm proposed in this paper is superior. As the number of spatial discrete points increases, the error gradually decreases, and the convergence order approaches the sixth order. Additionally, the numerical solution exhibits good stability at different spatial resolutions. Figure 4 shows the error situation at each discrete point when the spatial step size h is set to 1, 0.5, 0.25, and 0.125, at time t = 1.

Table 3. Comparison of numerical solutions and exact solutions for different spatial step sizes.

x	Numerical solutions			Exact solutions
	$h = 0.5$	$h = 0.25$	$h = 0.125$	
-2	0.195570341839716	0.195570317837384	0.195570317498287	0.195570317493043
1	0.669761714960261	0.669761551833839	0.669761549365509	0.669761549326657
4	0.944192776812420	0.944192780723502	0.944192780791714	0.944192780792830
7	0.992964649799372	0.992964648928960	0.992964648915042	0.992964648914826
10	0.999151394949809	0.999151395035921	0.999151395037261	0.999151395037289
13	0.999898198917428	0.999898198931662	0.999898198931886	0.999898198931891
16	0.999987795679827	0.999987795681589	0.999987795681621	0.999987795681621
19	0.999998537012758	0.999998537012975	0.999998537012976	0.999998537012976
22	0.999999824626747	0.999999824626765	0.999999824626763	0.999999824626765

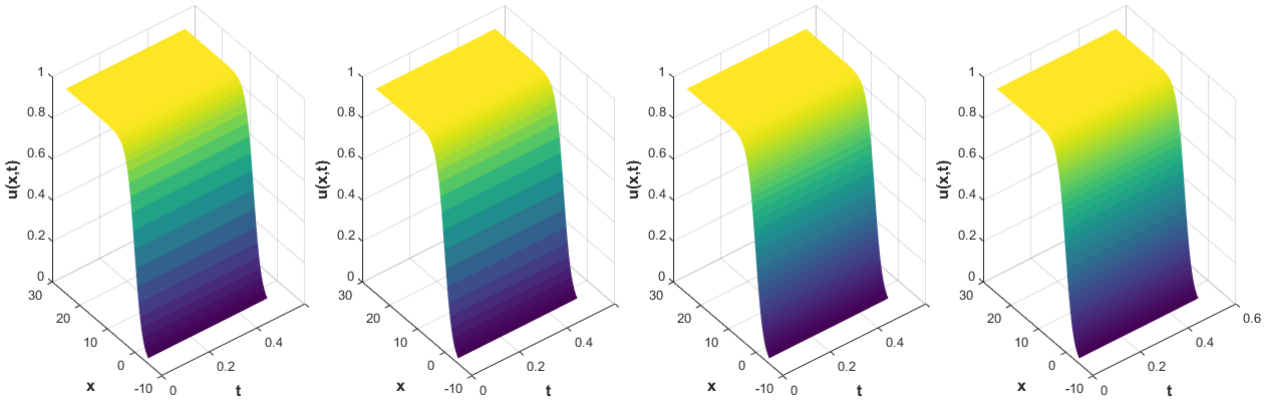

(a) Numerical, $h = 0.5$ **(b)** Exact, $h = 0.5$ **(c)** Numerical, $h = 0.25$ **(d)** Exact, $h = 0.25$

Figure 3. Comparison of numerical and exact solutions for different h.

Table 4. Comparison of the L_2 errors, L_∞ errors, and convergence order of different algorithms.

h	backward Euler method		the algorithm of the [17]		the algorithm in this paper	
	L_∞	order	L_∞	order	L_∞	order
1	9.5178×10^{-4}	–	7.0569×10^{-5}	–	1.1797×10^{-5}	–
0.5	2.4734×10^{-4}	1.9441	4.1635×10^{-6}	4.0832	1.6565×10^{-7}	6.1542
0.25	6.3067×10^{-5}	1.9716	2.5620×10^{-7}	4.0225	2.6608×10^{-9}	5.9601
0.125	1.5770×10^{-5}	1.9997	1.5949×10^{-8}	4.0057	4.1168×10^{-11}	6.0142
0.0625	3.9516×10^{-6}	1.9966	9.9584×10^{-10}	4.0014	6.5337×10^{-13}	5.9775

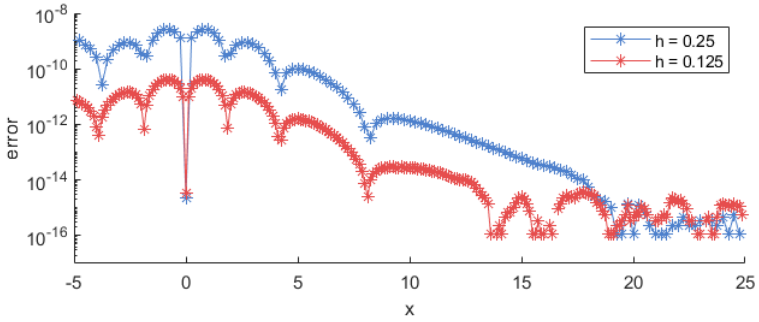

Figure 4. Numerical errors of discrete points with different M values at time t=1.

6. Conclusions

In this paper, a novel high-precision compact finite difference algorithm was developed to solve nonlinear reaction-diffusion equations, with a specific application to the FHN equation. The spatial second-order derivatives were discretized using a sixth-order compact finite difference scheme, while the time integration was performed using a semi-implicit Crank-Nicolson method. Through two numerical experiments, the numerical results obtained by this method were found to be basically consistent with the exact solution. Compared with other algorithms, it has a higher algorithmic accuracy, achieving sixth-order spatial convergence accuracy, which can maintain high accuracy at lower grid resolutions and save computational resources. Moreover, the method proposed in this paper can be extended to solve other nonlinear reaction-diffusion equations, which makes it an effective tool to solve numerical solutions of such partial differential equations and helps to better understand the behavior of biological systems.

Author contributions

Jiang Fu: Software, Validation, Visualization, Methodology, Writing–original draft; Xiao-yu Zhang: Supervision, Funding acquisition, Project administration, Writing–review & editing; Qing Fang: Conceptualization, Resources, Methodology. All authors have read and agreed to the published version of the manuscript.

Use of Generative-AI tools declaration

The authors declare they have not used Artificial Intelligence (AI) tools in the creation of this article.

Acknowledgments

This research was supported by the Ministry of Science and Technology of China under the National Key Research and Development Program (Sub-project, Grant No. 2021YFB2301601).

Conflict of interest

The authors declare no conflicts of interest.

References

1. Q. Xu, X. J. Chen, B. Chen, H. G. Wu, Z. Li, H. Bao, Dynamical analysis of an improved FitzHugh-Nagumo neuron model with multiplier-free implementation, *Nonlinear Dyn.*, **111** (2023), 8737–8749. https://doi.org/10.1007/s11071-023-08274-4
2. J. Bisquert, A frequency domain analysis of the excitability and bifurcations of the FitzHugh-Nagumo neuron model, *J. Phys. Chem. Lett.*, **12** (2021), 11005–11013. https://doi.org/10.1021/acs.jpclett.1c03406
3. H. Bao, W. B. Liu, M. Chen, Hidden extreme multistability and dimensionality reduction analysis for an improved non-autonomous memristive FitzHugh-Nagumo circuit, *Nonlinear Dyn.*, **96** (2019), 1879–1894. https://doi.org/10.1007/s11071-019-04890-1
4. A. R. Seadawy, S. T. R. Rizvi, S. Ahmed, Multiple lump, generalized breathers, Akhmediev breather, manifold periodic and rogue wave solutions for generalized Fitzhugh-Nagumo equation: applications in nuclear reactor theory, *Chaos Solitons Fract.*, **161** (2022), 112326. https://doi.org/10.1016/j.chaos.2022.112326
5. R. FitzHugh, Impulses and physiological states in theoretical models of nerve membrane, *Biophys. J.*, **1** (1961), 445–466. https://doi.org/10.1016/s0006-3495(61)86902-6
6. J. Nagumo, S. Arimoto, S. Yoshizawa, An active pulse transmission line simulating nerve axon, *Proc. IRE*, **50** (1962), 2061–2070. https://doi.org/10.1109/jrproc.1962.288235
7. G. Hariharan, K. Kannan, Haar wavelet method for solving some nonlinear Parabolic equations, *J. Math. Chem.*, **48** (2010), 1044–1061. https://doi.org/10.1007/s10910-010-9724-0
8. M. Namjoo, S. Zibaei, Numerical solutions of FitzHugh-Nagumo equation by exact finite-difference and NSFD schemes, *Comput. Appl. Math.*, **37** (2018), 1395–1411. https://doi.org/10.1007/s40314-016-0406-9
9. H. S. Shekarabi, M. Aqamohamadi, J. Rashidinia, Tension spline method for solution of FitzHugh-Nagumo equation, *Trans. A. Razmadze Math. Inst.*, **172** (2018), 571–581. https://doi.org/10.1016/j.trmi.2018.02.001
10. B. İnan, A finite difference method for solving generalized FitzHugh-Nagumo equation, *AIP Conf. Proc.*, **1926** (2018), 020018. https://doi.org/10.1063/1.5020467
11. B. İnan, K. K. Ali, A. Saha, T. Ak, Analytical and numerical solutions of the FitzHugh-Nagumo equation and their multistability behavior, *Numer. Methods Partial Differ. Equ.*, **37** (2021), 7–23. https://doi.org/10.1002/num.22516
12. G. A. Al-Juaifri, A. J. Harfash, Finite element analysis of nonlinear reaction-diffusion system of FitzHugh-Nagumo type with Robin boundary conditions, *Math. Comput. Simul.*, **203** (2023), 486–517. https://doi.org/10.1016/j.matcom.2022.07.005
13. K. M. Agbavon, A. R. Appadu, Construction and analysis of some nonstandard finite difference methods for the FitzHugh-Nagumo equation, *Numer. Methods Partial Differ. Equ.*, **36** (2020), 1145–1169. https://doi.org/10.1002/num.22468
14. N. Hilal, S. Injrou, R. Karroum, Exponential finite difference methods for solving Newell-Whitehead-Segel equation, *Arab. J. Math.*, **9** (2020), 367–379. https://doi.org/10.1007/s40065-020-00280-3

15. Z. Y. Fan, K. K. Ali, M. Maneea, M. Inc, S. W. Yao, Solution of time fractional FitzHugh-Nagumo equation using semi analytical techniques, *Results Phys.*, **51** (2023), 106679. https://doi.org/10.1016/j.rinp.2023.106679
16. S. K. Lele, Compact finite difference schemes with spectral-like resolution, *J. Comput. Phys.*, **103** (1992), 16–42. https://doi.org/10.1016/0021-9991(92)90324-r
17. D. P. Gui, A fourth-order compact finite difference scheme to the numerical solution of FitzHugh-Nagumo equation, *Appl. Mech. Mater.*, **873** (2017), 337–341. https://doi.org/10.4028/www.scientific.net/amm.873.337

AIMS Press